Organic photolysis reactions in tropospheric aerosols: Effect on secondary organic aerosol formation and lifetime

Hodzic A.[1], Madronich S.[1], Kasibhatla P.S.[2], Tyndall G.[1], Aumont B.[3], Jimenez J.L.[4], Lee-Taylor J.[1], Orlando J.[1]

[1]*National Center for Atmospheric Research, Boulder, CO, USA*

[2]*Nicholas School of the Environment, Duke University, Durham, USA*

[3]*LISA UMR CNRS 7583, Université Paris Est Créteil et Université Paris Diderot, France*

[4]*University of Colorado, Boulder, CO, USA*

Correspondence to A. Hodzic ***alma@ucar.edu***

To be submitted to ACP

Key words: secondary organic aerosol, photolysis rates, photo-fragmentation

Abstract

This study presents the first modeling estimates of the potential effect of gas- and particle-phase organic photolysis reactions on the formation and lifetime of secondary organic aerosols (SOA). Typically only photolysis of smaller organic molecules (e.g. formaldehyde) for which explicit data exist is included in chemistry-climate models. Here, we specifically examine the photolysis of larger molecules that actively partition between the gas and particle phases. The chemical mechanism generator GECKO-A is used to explicitly model SOA formation from α-pinene, toluene, and C_{12} and C_{16} n-alkane reactions with OH at low- and high-NOx. Simulations are conducted for typical mid-latitude conditions and a solar zenith angle of 45° (permanent daylight). The results show that after four days of chemical aging under those conditions (equivalent to eight days in the summer mid-latitudes), gas-phase photolysis leads to a moderate decrease in SOA yields i.e ~15% (low-NOx) to ~45% (high-NOx) for α-pinene, ~15% for toluene, ~25% for C_{12}-alkane, and ~10% for C_{16}-alkane. The small effect of gas phase photolysis on low volatility n-alkanes such as C_{16}-alkane is due to the rapid partitioning of early-generation products to the particle-phase where they are protected from gas-phase photolysis. Minor changes are found in the volatility distribution of organic products and in oxygen to carbon ratios. The decrease in SOA mass is increasingly more important after a day of chemical processing, suggesting that most laboratory experiments are likely too short to quantify the effect of gas-phase photolysis on SOA yields. Our results also suggest that many molecules containing chromophores are preferentially partitioned into the particle phase before they can be photolyzed in the gas-phase. Given the growing experimental evidence that these molecules can undergo in-particle photolysis, we performed sensitivity simulations using an empirically estimated SOA photolysis rate of $J_{SOA}=4\times10^{-4}\ J_{NO2}$. Modeling results indicate that this photolytic loss rate would decrease SOA mass by 40-60% for most species after ten days of equivalent atmospheric aging at mid-latitudes in the summer. It should be noted that in our simulations we do not consider in-particle or aqueous-phase reactions which could modify the chemical composition of the particle, and thus the amount of photolabile species. The atmospheric implications of our results are significant for both the SOA global distribution and lifetime. GEOS-Chem global model results suggest that particle-phase photolytic reactions could be an important loss process for SOA in the atmosphere, removing aerosols from the troposphere on timescales of less than 7 days that are comparable to wet deposition.

1 Introduction

Secondary organic aerosols (SOA) are ubiquitous atmospheric constituents formed by photochemical oxidation of anthropogenic and biogenic hydrocarbons that can lead to adverse health effects (*Fann et al., 2012*) and radiative forcing of climate (*Boucher et al., 2013*). Their atmospheric burden and lifetime are highly uncertain due to our limited understanding of processes controlling their formation, aging and removal in the atmosphere. SOA yields and the volatility distribution of intermediate oxidation products greatly depend on the competitive chemistry of peroxy radicals (RO_2) formed from oxidation of parent hydrocarbons, which can react with nitrogen oxides (NO), hydroperoxy radicals (HO_2), or other RO_2 (*Ziemann and Atkinson, 2012*). The resulting oxygenated molecules contain carbonyl, peroxide or nitrate chromophores, and are potentially sensitive to photolysis during their lifetime in the atmosphere (*Finlayson-Pitts and Pitts, 2000*). Photolysis can occur in the gas-phase and in the condensed phase as particles containing photolabile compounds efficiently absorb light at actinic wavelengths (*e.g. Lambe et al., 2013; Wong et al., 2014*). Unlike OH reactions that mainly lead to addition of more functional groups, photolysis mainly fragments molecules into smaller and more volatile compounds thus significantly modifying SOA composition and properties during atmospheric aging.

Evidence that photolysis modulates SOA formation and lifetime in the atmosphere is supported by a growing number of laboratory experiments, which showed that exposure to UV lights can suppress SOA formation or even cause substantial loss of biogenic SOA. Presto et al. (*2005*) observed a 20-40% decrease in aerosol yields during α-pinene ozonolysis experiments conducted under UV lights. Zhang et al. (*2006*) found similar sensitivity to UV exposure for d-limonene ozonolysis SOA, with a mass yield decrease of 60% for compounds with saturation concentration of 1 μg m^{-3}. In both cases, the SOA decrease was attributed to the photolysis of gas-phase intermediates during the active growth phase and changes in their volatility distribution. Specific

SOA aging experiments were also performed to isolate the effect of photolysis from other processes (*e.g. Tritscher et al., 2011; Salo et al., 2011; Henry and Donahue, 2012; Donahue et al., 2012*). In those experiments, SOA was first formed from α-pinene ozonolysis in the dark, and then the products were irradiated (with UV lamps or solar lights), which allowed separation of the aging by OH-radical oxidation and photolysis from the initial condensation of primary products. Henry and Donahue (*2012*) reported a strong photolytic loss of 6×10^{-5} s^{-1} of the formed SOA mass upon UV 360nm black-light exposure with lower OH levels (~10^6 molecules cm^{-3}) via H_2O_2 photolysis. In additional experiments reported by Donahue et al. (*2012*), where OH was formed via HONO photolysis, an initial increase in SOA concentrations was first observed, followed by their strong decrease as OH concentrations dropped from 10^7 to 10^6 molecules cm^{-3}. The authors attributed this SOA loss to photolysis in the gas-phase followed by particle-to-gas re-equilibration, under the assumption that particle-phase quantum yields of photodissociation are small due to quenching and cage effects from neighboring molecules. However, recent studies that were able to decouple gas-phase and condensed-phase processes seem to suggest a rapid photolytic loss of SOA in the condensed phase. Epstein et al. (*2014*) irradiated α-pinene ozonolysis SOA denuded from gas-phase oxidants and organic vapors, and concluded that condensed-phase photolysis was responsible for a significant decrease in SOA mass caused by the photochemical loss of particle-bound peroxide species (a 50% loss over 1 equivalent week in the atmosphere). Wong et al. (*2014*) also reported a substantial photolytic loss of α-pinene SOA mass (generated by re-atomization after sampling into filters) under UVB lights with loss rates of 7.9×10^{-5} s^{-1} under dry conditions and a 2x faster loss (1.6×10^{-4} s^{-1}) under higher relative humidities.

During photochemical aging in the atmosphere, SOA can be both generated by oxidative functionalization with OH, and destroyed by photolysis. As these processes are occurring simultaneously and during the entire organic aerosol (OA) lifecycle in the atmosphere (typically a

105 week), it is currently challenging to quantify separately the effect of photolysis on SOA yields
106 and aging from laboratory experiments, and to describe their effect in the models. To our
107 knowledge, photolysis of oxygenated organic molecules in the gas- or condensed-phase is
108 ignored in most current chemistry-climate models, which could result in substantial errors in SOA
109 predictions. In addition, the experimental quantification of SOA photolytic loss could be
110 significantly biased due to SOA evaporation caused by heating inside the chamber upon UV light
111 exposure (*Denjean et al., 2014*).

112 The objective of the present study is to examine the effect of both gas- and condensed-phase
113 photolysis on SOA formation and lifetime using process and global modeling. First, we study the
114 multi-day growth of SOA from four typical precursors (α-pinene, toluene, and semi-volatile and
115 intermediate volatility n-alkanes) under idealized conditions (constant fixed daylight,
116 temperature, OH, NOx, O_3, and preexisting OA) to assess the maximum potential impact of
117 photolysis on SOA formation. The mechanism generator GECKO-A is used to create explicit
118 oxidation schemes for these precursors, which are then run within a box model to assess the effect
119 of photolysis on SOA yields under a range of conditions. The effect of gas-phase photolysis is
120 explicitly quantified in the box model, whereas the potential role of in-particle photolysis is
121 empirically estimated and discussed based on sensitivity simulations. We then include a
122 simplified parameterization of photolysis reactions within a global chemistry model to estimate
123 the potential effect of photolysis on ambient SOA under realistic conditions involving spatial and
124 temporal variability in SOA precursor emissions and chemistry, and in the presence of other
125 competing SOA loss processes.

126 ## 2 Modeling framework

127 The mechanism self-generator GECKO-A (Generator of Explicit Chemistry and Kinetics of
128 Organics in the Atmosphere) was used in this study to create the detailed gas-phase oxidation
129 mechanisms for individual SOA precursors including α-pinene, toluene, and C_{12} and C_{16} n-

alkanes. The chemical mechanisms are created using a prescribed set of rules determining reaction pathways and rate coefficients, based on laboratory kinetic data, and structure-activity relationships as described by Aumont et al. (*2005*). The protocol currently implemented in GECKO-A allows the generation of chemical mechanisms for aliphatic species only. For aromatic species (i.e toluene in this study), the mechanism is taken from the Master Chemical Mechanism (MCM) (*Jenkin et al., 2003*) up to the formation of ring opening products, where mechanism generation by GECKO-A is next used. Rate coefficients for reaction of OH with organics are based on structure-reactivity rules of Kwok and Atkinson (*1995*) and subsequent updates. In this study, we have updated the rate constants for H-atom abstraction from carbon atoms containing a hydroperoxide functionality (e.g., RC-H(OOH)R). Kinetic data for OH / hydroperoxide reactions are sparse in the literature, and previous versions of GECKO-A assumed an activation factor (i.e. an enhancement of the rate constant due to the presence of the functional group) of 14 on the basis of data for the OH/CH_3OOH reaction. That is, the presence of the –OOH group was assumed to increase the reactivity of the adjacent C-H bond(s) by this factor. We have changed this factor to 3.5 similar to that for –OH (Atkinson R. personal communication), and discuss its effect on our results in section 3.1. The choice of a lower activation factor is supported by measurements of gas-phase dodecyl hydroperoxides in the work of Yee et al. (*2012*), who found that the loss of these peroxides was much too fast when using the MCM value based on a large value of F(-OOH). For the gas-particle partitioning, instantaneous equilibrium is assumed, and the Nannoolal et al. (*2008*) approach is used to estimate the saturation vapor pressure for non-radical species. The fraction that is partitioned to the particle phase can be determined as $F_{aerosol,i} = \left(\frac{C_{OA}}{C_{OA}+C_i^*}\right)$ where C_{OA} is the aerosol mass concentration (µg m^{-3}), and C_i^* is an effective saturation mass concentration (µg m^{-3}). The gas/particle equilibrium and the composition of SOA are constantly modified as the gas-phase oxidation progresses during the atmospheric aging. Condensed-phase reactions are not considered, nor are potential diffusion

limitations to SOA partitioning. Gas-phase photolytic reactions are included for molecules containing carbonyl, hydroperoxide or nitrate chromophores. For species containing several functional groups, each chromophore is treated independently, except for conjugated carbonyls. The photolysis of nitroaromatic compounds is not included. To determine the associated photolysis rates, each molecular structure predicted by GECKO-A is assigned a reference compound with its associated cross sections and quantum yields as described by Aumont et al. (*2005*, see Table 4). SI-Table 1 summarizes the photolysis rates for chromophores and molecular structures that are considered in GECKO-A. Particle-phase photolysis is not explicitly calculated in the default model, and sensitivity simulations will be preformed in this study to quantify its effects as discussed in section 3.2.

In this study simulations are performed in a box model with the prescribed conditions representative of ambient air as in the study by Hodzic et al. (*2014*) to quantify the effect of photolysis on SOA formation and yields. In these runs, temperature is set to 298K, photolysis frequencies are calculated for mid-latitudes at a solar zenith angle of 45° (J_{NO2} = 8.1×10^{-3} s^{-1} which corresponds to a constant daylight), NO_X levels are held at 0.01 ppb for low and 10 ppb for high-NOx conditions, ozone is set at 40 ppb, and OH is kept constant at 2×10^{6} molecules cm^{-3}. The pre-existing OA concentration is 10 μg m^{-3}, typical of moderately polluted conditions. Sensitivity simulations with higher OH values (8×10^{6} molecules cm^{-3}) or lower pre-existing OA (1 μg m^{-3}) are also performed. The initial hydrocarbon mixing ratio is fixed to an arbitrary low value of 1 ppt, so that the amount of aerosol produced from the given precursor is negligible compared to preexisting OA prescribed in the study and will not impact the gas/particle partitioning, nor the overall photochemical reactivity. Under these conditions, SOA yields are independent of the amount of initial precursor as discussed by Hodzic et al. (*2014*). SOA yields and volatility distribution of intermediate products depend to a large extent on the relative rates of RO_2+HO_2 and RO_2+RO_2 (minor) versus RO_2+NO reactions. We calculated that 8% of RO_2

reactions proceed with NO under "low-NOx" vs. 99.9% under "high-NOx" conditions considered in this study.

We define the *Photolysis Age* in J_{NO2} equivalent days (Table 1) as the J_{NO2} exposure of the simulated SOA during our simulations normalized to a 1 day average summer (or winter) J_{NO2} exposure: $Photolysis\ Age = \frac{(J_{NO2} \times time)}{J_{NO2\_average}}$ where *time* is the duration of the simulation in days. Photolysis Age values are reported in Table 1 for our experiments. Typically, our 1 week simulations performed under constant lights at mid-latitudes and a solar zenith angle of 45° (J_{NO2} = 8.1×10^{-3} s^{-1}) are equivalent to about 2 equivalent weeks of exposure in the atmosphere at mid-latitudes during summer, or to about 38 equivalent days during winter.

3 Results and discussion

3.1 Importance of gas-phase photolysis of organics

To investigate the role of gas-phase photolysis on SOA formation and yields, we compared experiments with photolysis on and off for four typical SOA precursors including α-pinene, toluene, and C_{12} and C_{16} n-alkanes (Table 2). In the "photolysis off experiment" photolysis of all organic species (except for formaldehyde and methylhydroperoxide) is turned off, whereas all inorganic compounds (i.e. O_3, NO_2, NO_3, H_2O_2, HONO, HNO_3, HNO_4) still undergo photolysis. Figure 1 shows the results for two different levels of NO_X (0.01 ppb and 10 ppb), OH ($2x10^6$ and $8x10^6$ molecules cm^{-3}) and background OA (1 and 10 μg m^{-3}). BASE case simulations with and without photolysis of organics are shown in black. The results indicate that in a week of chemical aging with constant daylight or two weeks of equivalent atmospheric summertime exposure (representative of Boulder 40°N with the solar zenith angle of 45°) the gas-phase photolysis leads to a 10 to 45% decrease in SOA concentrations depending on the precursor. Most of the decrease occurs in the first 4 days of the simulation (8 equivalent atmospheric days). For a given species, the sensitivity to gas-phase photolysis is comparable under low- and high-NO_X conditions, except

for α-pinene SOA, which seems to be more sensitive under high-NO_X. Our results also suggest that for most species the resulting loss of SOA due to gas-phase photolysis is increasingly more important as the chemical processing time is increased during the first week atmospheric exposure (Figure SI-1).

The largest effect on yields (Table 3) is predicted for α-pinene SOA, with a reduction of 16% under low-NOx and 47% under high-NOx during the entire experiment. The reduction is relatively small during the initial 10 hours, which is a typical duration of laboratory experiments, with a 2% decrease at low-NOx (10% high-NOx), and reaches ~5% (20%) after 1 day, or 12% (42%) after one week of equivalent atmospheric ageing. For toluene oxidation, the effect of photolysis is more limited, and does not exceed 15% for either low- or high-NOx conditions. We note however that the effect could be underestimated as the photolysis of nitroaromatic compounds, which are strong absorbers, is currently not represented in GECKO-A. For products of n-alkanes, the relative decrease in SOA yields is ~10% for C_{16} n-alkanes and ~25-30% for C_{12} n-alkane. The sensitivity to gas-phase photolysis is more important for C_{12} than C_{16} n-alkane, due to the fact that products of C_{16} n-alkane are partitioned to the particle-phase in a much greater fraction after one generation of chemistry where they are protected from gas-phase photolysis, whereas it takes several generations to produce substantial SOA from shorter chain n-alkanes (*Aumont et al., 2012*).

The efficiency of the gas-phase photolysis will depend on the residence time of organic vapors in the gas-phase, which can be significantly modified by the chemical environment. For instance, an increase in the OA mass available for the gas/particle partitioning is expected to enhance the partitioning of organics to the condensed phase where they will be protected from gas-phase photolysis. Similarly, a faster gas-phase oxidation rate (higher OH) is expected to lead to more rapid generation of the low volatility organic species which can condense into the particle-phase thus making them less vulnerable to the gas-phase photolysis. Sensitivity simulations with 4-

times higher OH concentrations (SENS_OH) and 10-times lower background OA (SENS_OA) are performed to evaluate these effects (Figure 1). As expected, SOA formation occurs more rapidly when a 4-fold increase in OH is considered. The decrease by an order of magnitude in the amount of the pre-existing OA (and thus reduced gas/particle partitioning) also affects the amount of SOA formed. A large (~75%) decrease in SOA production is observed for toluene because a significant fraction of the predicted oxidation products have effective saturation mass concentrations (C*) in the 1-10^3 μg m^{-3} range (Figure 4, see also Hodzic et al. (*2014*)). The effect is more limited for SOA produced from other precursors (up to 30%). For all precursor species, the sensitivity to photolytic reactions remains qualitatively similar (within 10%) regardless of the OH and OA background values (Figure SI-1). As expected, a decrease in background OA concentrations leads in most cases to an enhancement of the SOA photolytic loss, whereas an increase in OH levels tends to result in a reduced SOA photolytic removal. We also note that the sensitivity to gas-phase photolysis is not significantly modified when diurnally variable photolysis rates are considered instead of fixed constant daylight conditions (see Figure SI-3).

Figure 2 shows the major functional groups in SOA molecules from various precursors. Fifteen families of functional groups are considered and they account for 54% to 65% of the total SOA mass for α-pinene, 94% to 99% for toluene, and for 70% to 90% for C_{12} and C_{16} n-alkanes. Positional isomers are lumped into the same family of compounds. Ketone (K) and alcohol (O) moieties are present in a majority of the molecules, while hydroperoxides (H) are seen mainly at low NO_X and nitrates (N) mainly at high NO_X. Gas-phase photolysis leads to a decrease in most species, which seems to be particularly important for highly functionalized compounds containing multiple carbonyl and nitrate groups (e.g. HKKKK, HHKK, HHKKK, HKKK, NNKK, NNKO where e.g. HHKK refers to a molecule that contains two hydroperoxide and two ketone groups). These species are formed by several generations of chemistry and are mainly found in the particle-phase. Thus their decrease is more likely related to reductions in their precursor species

255 due to photodegradation than to their direct loss by gas-phase photolysis. Some molecules
256 containing alcohol groups (e.g. HHO, HKKO, HHKO) see an increase in their concentrations due
257 to gas-phase photolysis (see also Figure SI-2). This increase can be explained by photolysis of
258 hydroperoxides, which can lead to the formation of alkoxy radicals that can isomerize to form
259 alcohols. Thus photolysis can both contribute to SOA loss and to a lesser extent to its formation.
260 Typically, photolysis of carbonyl compounds (ketone and aldehydes) tends to break the α-carbon
261 bond on either side of the C=O group, leading to smaller more volatile fragments, that are less
262 likely to partition to the particle-phase. On the other hand, photolysis of hydroperoxides and
263 nitrates leads to elimination of -OH or -NO_2, leading to alkoxy radicals, and potentially further
264 functionalization of the carbon skeleton favoring formation of less volatile organic compounds,
265 that can partition more readily to the particle.

266 One of the highly uncertain factors that can influence the composition of SOA at low- NO_X is the
267 choice of the rate for abstracting the H atoms from the carbon atom that is adjacent to the
268 hydroperoxide (-OOH) group. As discussed in Section 2, in this paper we have used a lower
269 activation factor of 3.5 for estimating the rate constant of that process, instead of the GECKO-A
270 default value of 14 (*Aumont et al., 2005*). As shown in Figure SI-4 this change doesn't affect the
271 SOA production when the gas-phase photolysis of organics is turned off (~8 μg m^{-3} for C_{12} n-
272 alkane). However, the composition of SOA formed from n-alkanes is significantly modified, as is
273 the effect of gas-phase photolysis on SOA yields (~ 2x smaller when the value of 3.5 is
274 considered). The main difference is found for HKKKK and HKKK molecules which are much
275 more abundant when the value of 14 is used. These molecules originate typically from the
276 successive OH reaction, leading to an hydroperoxide moieties under low-NO_X condition and their
277 subsequent fast oxidation to a ketone moiety due to a the large activation factor used. Reducing
278 this factor to 3.5 forces the OH to react away from the -OOH group. When the carbon backbone
279 is sparsely functionalized, this increases the rate of production of multifunctional species, in

280 particular multifunctional peroxydes (e.g. HHO et HHK). However, when the carbon backbone is
281 highly functionalized, this leads to more fragmentation, because in most cases the OH attack is
282 now next to other functional moieties (e.g. multifunctional ketones).

283 Figure 3 shows the effect of gas-phase photolysis on oxygen to carbon (O/C) ratios of particles
284 for the BASE run. For all cases, changes in O/C ratios (<0.05) are minor. Slightly higher O/C
285 ratios at low NO_X were found in the presence of gas-phase photolysis as photolyzed fragments are
286 typically smaller and more volatile carbon chains that need to undergo further oxidation to
287 condense into particles. Our results are consistent with chamber studies by Wong et al. (*2014*)
288 that observed small changes in O/C with an increase in more oxidized compounds (high O/C) in
289 α-pinene SOA due to fast photodegradation of less oxidized particulate organics such as
290 carbonyls. Changes in SOA composition due to gas-phase photolysis can also affect the volatility
291 distribution of oxidized organic compounds. Figure 4 doesn't show a clear shift in volatility due
292 to gas-phase photolysis, but rather suggests that the SOA reduction is happening across a wide
293 range of volatility bins.

294 Our explicit modeling results suggest that gas-phase photolysis leads in some cases to moderate
295 changes in SOA yields (<25% for most precursors; <45% for high-NO_X α-pinene), and small
296 changes in volatility distribution and O/C ratios over 1 equivalent week of chemical aging in the
297 mid-latitude atmosphere in summer or 2.5 weeks in winter. The implication in terms of SOA
298 atmospheric lifetime is that gas-phase photolysis is a possible sink of intermediate organic vapors
299 and thus SOA, although a smaller sink compared to dry deposition of these gaseous species
300 (*Hodzic et al., 2014, Knote et al., 2014*). Indeed, the estimated summertime atmospheric lifetimes
301 against photolysis of the SOA from the four precursors considered in our study range from about
302 10 days for α-pinene under high-NO_X conditions (unlikely case), to more than a month for α-
303 pinene under low-NO_X conditions or for long chain n-alkane species. These lifetimes are
304 considerably longer than values reported by laboratory studies (*e.g. Henry and Donahue, 2012*).

Current 3D models typically represent the oxidation products as lumped surrogate species based on their volatility that can further age by OH oxidation but cannot photolyze due to the undefined chemical structure of those intermediate species. Our results suggest that omitting their gas-phase photolysis will likely result in reasonably small biases in SOA predictions over urban scales. However, errors could be significant at the global scale in particular in the upper troposphere where models have the tendency to accumulate SOA due to a less efficient wet removal.

3.2 Importance of in-particle photolysis of organics

In the GECKO-A simulations described above, once the organic molecules are partitioned to SOA they are protected from gas-phase photolysis. However, these molecules still contain numerous chromophores (Figure 2) that absorb solar radiation, and could undergo photolysis inside the particle. Optical absorption is also likely to be modified by the heterogeneous formation of high molecular weight compounds inside the particle (*Graber and Rudich, 2006*). As GECKO-A does not include condensed-phase photochemical reactions (or heterogeneous chemistry), the effect of particle-phase photolysis on SOA cannot be calculated directly. In this section, we consider a simple alternative empirical approach to examine the potential effect of particle-phase photolysis within GECKO-A.

We base our estimates of condensed-phase photolysis on measured SOA mass absorption coefficient (*MAC*). Organic particles containing photolabile compounds have been shown to efficiently absorb light at actinic wavelengths. Recently measured *MAC* values range from 0.03 to 0.5 m^2g^{-1} for laboratory data (*Lambe et al.,* 2013) or from 0.1 to 10 m^2g^{-1} for ambient urban measurements (e.g. *Barnard et al., 2008*) in the 300-400 nm wavelength interval. We use those measurements to estimate the condensed-phase photolysis of SOA. We represent the photolytic SOA loss as a first order reaction, with effective reaction rate coefficient J_{SOA}:

$$J_{SOA} = [AF] \times [MAC] \times [mc] \times [QY] \quad (1)$$

where *AF* is the actinic flux (photons m^{-2} s^{-1}), *MAC* is the SOA mass absorption coefficient (m^2 g^{-1}), *mc* is the mass of one carbon atom (g) and *QY* is the quantum yield or the probability that absorbed photons will lead to bond cleavage and the loss of some mass from the particle. We assume that if each absorbed photon leads to the loss of one C atom, the quantum yield is equal to one. We can scale (1) to known NO_2 photolysis:

$$J_{SOA} = J_{NO2} \times [AF/J_{NO2}] \times [MAC] \times [mc] \times [QY] \quad (2)$$

The photolysis model TUV (v5.1, (*Madronich et al. 1993*)) was used to estimate the UV actinic flux (= 2×10^{20} photons m^{-2} s^{-1}) and NO_2 photolysis (= 9.7×10^{-3} s^{-1}) over 280-400 nm at 1 km altitude and overhead sun, which combined with [mc] gives $[AF/J_{NO2}] \times [mc] = 0.4$ photons g m^{-2}. Thus the resulting SOA photolysis rate can be written as:

$$J_{SOA} = 0.4 \times J_{NO2} \times [MAC] \times [QY] \quad (3)$$

To estimate the plausible range of J_{SOA} values, we use the combinations of [MAC] x [QY] reported in the literature. Here we use *MAC* of 0.1 m^2g^{-1} as a lower limit for ambient aerosols. We note that for the chosen MAC value the light can penetrate the whole volume of the particle without being significantly attenuated by the absorbers (light attenuation was estimated to be less than 2-3%, see discussion SI Annex IV). *QY* has only been measured for a handful of species. Calvert and Pitts (*1966*) reported values of 0.01 (or 1%) for photolysis of aldehydes in the aqueous phase. Lignell et al. (*2013*) reported values of 0.5 for cis-pinonic acid, which is one of the constituents of α-pinene SOA, whereas Wong et al. (*2014*) estimated an effective quantum yield of 1.2±0.2 for the loss of organics in the case of α-pinene SOA photolysis. Given the range of values, here we use a conservative value of 0.01 (or 1%) for *QY*. Thus our best estimate for J_{SOA} is 0.04% of J_{NO2}. This value of J_{SOA} is applied as a first order removal rate for each photolabile species in the particle phase. The photo fragments are not longer considered and the condensed phase photolysis is here considered as an irreversible loss of one carbon atom. We note that this calculated value is 1-2 order of magnitude lower that those reported by Henry and

354 Donahue (*2012*) who estimated the photolytic loss of SOA as 2% of J_{NO2} (total value of both
355 particle and gas-phase photolysis and J_{NO2} of 3×10^{-3} s^{-1}). In their experiments, Henry and
356 Donahue (*2012*) argued that photolysis is more efficient (higher QY) in the gas-phase than in the
357 particle phase where quenching and caging are more likely to occur and could cause rapid
358 recombination of fragments. Therefore a lower *QY* may be expected in the particles, although it is
359 unclear whether similar molecules are involved in photolysis in the two phases. We also note that
360 photolysis of SOA is assumed to not occur at visible wavelengths (i.e. QY = 0 for $\lambda > 400$ nm).

361 Figure 5 shows that considering the above estimated condensed-phase photolytic loss of SOA
362 ($J_{SOA} = 4\times10^{-4}\times J_{NO2} = 3.2\times10^{-6}$ s^{-1}; lifetime of 7 days at equivalent J_{NO2} atmospheric exposure, see
363 Table 1) in GECKO-A simulations leads to a 40-60% decrease in SOA mass after ten days of
364 equivalent atmospheric aging for most species (J_{mac} run, Figures 5 and SI-1). A more limited
365 decrease (15%) is found for the high-NOx toluene SOA because the photolytic loss of
366 nitroaromatic compounds, which are predicted to be the major SOA constituents (RVVO in
367 Figure 2), is not included.

368 For comparison, the effect of applying the gaseous photolysis rates for the corresponding species
369 in the condensed phase is shown in Figure 5 ($J_{molecmax}$). Similar to the simulations above based on
370 MAC, the photolysis is here again considered as an irreversible loss of organic carbon. The
371 comparison between J_{mac} and $J_{molecmax}$ shows a fairly similar (within 20%) reduction in SOA mass
372 for most precursors. The $J_{molecmax}$ run considers that chromophores and quantum yields are similar
373 in their gas and particle phase absorption, which is a crude assumption neglecting possible effects
374 form oligomerization, caging and quenching. In the absence of particle-phase chemistry, $J_{molecmax}$
375 could be viewed as an upper limit to photolysis effects, but changes in absorption with particle
376 aging complicate this simple interpretation as both enhancement and decrease in absorption have
377 been reported (e.g. *Shapiro et al., 2009; Bones et al., 2010; Updyke et al., 2012; Zhong and Jang,*
378 *2014*). In-particle reactions are likely to modify the chemical composition of the particle, and

379 therefore change the amount of photolabile species. For example, the work of Yee et al. (*2012*)
380 and Schilling-Fahnestock et al. (*2014*) indicate extensive formation of peroxyhemiacetals in the
381 SOA from dodecane oxidation at low NO_X. However, the precursor molecules are third and
382 fourth generation products, which contain additional, unfunctionalized ketone groups, which
383 would still be susceptible to photolysis.

384 The overall SOA loss rate due to the combined effect of gas- and particle-phase photolysis (and
385 ongoing OH chemistry) in GECKO-A runs was estimated for the J_{mac} simulations (see Table 4).
386 Values range between 3.1×10^{-6} and 5.6×10^{-6} s^{-1}, which translates to equivalent atmospheric SOA
387 lifetimes of 4 to 8 days with regard to photolysis in the summer, except for high-NO_X toluene
388 SOA with a lifetime of 20 equivalent summer days for which the effect of photolysis is likely
389 underestimated in our simulations as discussed above. The estimated SOA lifetime with regard to
390 photolysis is comparable or even shorter to the typical ~1 week aerosol atmospheric lifetime
391 which suggests that photolysis may be an important removal mechanism for atmospheric SOA.
392 Atmospheric implications of our findings are further investigated in section 3.3.

393 The above estimates for the α-pinene SOA photolytic loss rate cannot be directly compared with
394 those of Henry and Donahue (*2012*) and Wong et al. (*2014*) due to several factors including: (i)
395 the differences in the chemical composition of particles as the experiments typically use the SOA
396 pre-generated by α-pinene ozonolysis for short (few hours) exposure, whereas in our simulations
397 the SOA is generated mainly by OH oxidation, and over a much longer time period (> 1 week);
398 (ii) the possible evaporation of SOA in the laboratory experiments due to chamber heating under
399 the UV lamps, which was not quantified in those experiments and which does not occur in our
400 model simulations; (iii) in-particle chemistry that could modify the composition and absorption
401 properties of the SOA and which is not included in our model, and is generally not well
402 understood.

For comparison with previous laboratory work, we ran the model under conditions similar to Henry and Donahue (*2012*), in which α-pinene was oxidized by ozone in the dark in the presence of hydrogen peroxide, and then the mixture was exposed to UV black lights as in Presto et al. (*2005*) and/or to OH oxidation. Figure 6 shows the sensitivity of the aerosol mass to assumed photolysis rates for these conditions. The experiment is performed for 5 hours at the constant J_{NO2} of 3×10^{-3} s^{-1} which corresponds to 4 hours of equivalent summertime atmospheric exposure (Table 1). Our results show that when exposed to only OH reactions (photolysis of organics was turned off), SOA concentrations increase by ~35% in 5 hours of aging. On the other hand, SOA exposed to only photolytic reactions (no OH) decrease by ~7% over the simulation period. The combined effect of both photolytic and OH reactions is therefore an overall increase in SOA concentrations by ~30%. As done previously we also performed a sensitivity simulation in which all molecules can photolyze in both gas- and particle-phases at the gas-phase rate. Figure 6 shows that with those reactions the SOA concentrations are decreased by ~50% ($J_{molecmax}$) in 5 hours. These results suggest that most of the photolabile molecules are partitioned to the particle phase where they are protected from gas-phase photolysis. The corresponding loss rate due to the combined effect of gas- and particle-phase photolysis and OH oxidation, is 3.4×10^{-5} s^{-1}, which is within a factor of 2-3 of the values reported by Henry and Donahue (*2012*) and Wong et al. (*2014*).

3.3 Potential effect of photolysis on global SOA budget and lifetime

We implement the estimated SOA gas-phase and in-particle photolytic loss rates within the GEOS-Chem global chemistry model (*Bey et al., 2001*) to investigate the regional and global effect of photolytic reactions on SOA concentrations. The GEOS-Chem model configuration used in this study is described in detail by Jo et al. (*2013*). In particular, SOA is modeled using volatility basis set approach with aging in which oxygenated semi-volatile organic compounds (SVOC) formed by the gas-phase reaction of nine lumped hydrocarbon species (representing

monoterpenes, sesquiterpenes, isoprene, and aromatic compounds) with OH, O_3, and NO_3 are partitioned between gas and particle phases using 4 volatility bins (with saturation vapor pressures ranging from 1-1000 μg m^{-3} at 300K). Chemical aging of anthropogenic SVOC with OH (with a rate constant of $4x10^{-11}$ cm^3 $molecules^{-1}$ s^{-1}) is assumed to reduce the vapor pressure of the products by one order of magnitude. It should be noted that, similar to previous studies, gas-phase photolysis of these intermediate species is not included. Model simulations are performed for year 2009.

Figure 7 shows the annual mean SOA concentrations predicted by the default GEOS-Chem run within the lower troposphere (below 5 km). The predicted continental background levels of SOA typically vary between 0.2 and 0.4 μg m^{-3}, and the highest concentrations (>1.5 μg m^{-3}) are found over tropical forest regions of Africa and South America. Industrialized and urban areas in China, Europe and the U.S. feature SOA values significantly larger (0.5-1.5 μg m^{-3}) than the background. These SOA values and spatial distribution are consistent with previous studies (*e.g. Spracklen et al., 2011; Jo et al., 2013*). Our results (Figure 7b) suggest that gas-phase photolysis of intermediate semi-volatile organic compounds leads to a very small (< 4%) reduction in SOA concentrations under ambient conditions. A much larger impact on SOA concentrations is predicted for in-particle photolysis. When the previously estimated photolytic loss of 0.04% J_{NO2} is applied within the GEOS-Chem model, the annual mean SOA concentrations in the lower troposphere are decreased by ~20-30% over source regions, and up to 60% over remote regions (Figure 8a). The absolute decrease is ~0.3 μg m^{-3} over land and ~0.1 μg m^{-3} over oceans, with the highest absolute decrease of 0.6 μg m^{-3} coinciding with the maximum predicted SOA concentrations over Africa (Figure 7c). As the quantum yield of the particle-phase photolysis and mass absorption coefficients are highly uncertain, here we also consider an order of magnitude higher photolytic loss rate of 0.4% J_{NO2}. As shown in Figure 8c, this increase in J_{SOA} results in a larger reduction of SOA concentrations in the lower troposphere reaching 50-70% over land

surfaces, and up to 70-90% over water surfaces. In both cases, a strong spatial gradient is found between land and water surfaces, with larger relative reductions in SOA concentrations over oceans. This gradient is due to the continuous photolytic losses, the effect of which accumulates further away from source regions. Model results show that the relative decrease in SOA concentrations is ~20-30% stronger in the upper troposphere compared to the lower troposphere (Figure 8b,d).

Our results suggest that photolysis of SOA, which is currently ignored in chemistry-climate and air quality models, could be an efficient removal process for organic particles. The diagnosed SOA tropospheric lifetime against photolytic removal (annual-average tropospheric mass burden divided by the annual tropospheric loss due to photolysis) ranges from 1 day for J_{SOA}=0.4% J_{NO2} to 7 days for J_{SOA}=0.04% J_{NO2}, and is comparable to the lifetime associated with the SOA wet deposition which ranges from 3.5 to 5.5 days in these model runs. This photolytic loss pathway is expected to play a particularly important role in regions where wet deposition is not very efficient such as the upper troposphere and lower stratosphere.

4 Conclusions

In this study, we investigated the sensitivity of SOA formation and aging in the atmosphere to gas-phase and in-particle photolysis reactions of organic compounds that actively partition between gas and particle phases. We apply the explicit chemistry model GECKO-A to simulate SOA formation from OH oxidation of α-pinene, toluene, and C_{12} and C_{16} n-alkane precursors, and to explore the sensitivity of this formation to gas-phase photolysis explicitly calculated in the model. Our simulations are conducted for typical mid-latitude conditions (Boulder, CO) and a solar zenith angle of 45° under a week of permanent daylight. The results suggest that photolysis of intermediate organic compounds in the gas-phase leads to a moderate decrease in SOA yields i.e ~15% (low-NOx) to ~45% (high-NOx) for α-pinene, ~15% for toluene, ~25% for C_{12} n-alkane, and ~10% for C_{16} n-alkane during 8 days of equivalent atmospheric exposure in the

summer or 3 weeks in winter. This decrease depends on the aerosol chemical composition under various NO_X levels, and the amount of photolabile molecules. SOA formed from precursors considered here contained substantial amount of photolabile molecules, many of which were partitioned to the particle-phase before they could undergo gas-phase photolysis.

We performed sensitivity studies to estimate the potential effect of condensed-phase photolysis on SOA formation by applying an empirical J_{SOA} rate of $4\times10^{-4}\times J_{NO2}$ s^{-1} to formed particles. Our results suggest that condensed-phase photolysis might have a substantial effect on SOA formation and subsequent aging, with a decrease of 40-60% in SOA yields over ten days of equivalent atmospheric aging at mid-latitudes in the summer.

Explicit modeling of a typical α-pinene ozonolysis SOA aging experiment was also performed using GECKO-A. The results show a minor decrease (~7%) in SOA concentrations in 5 hours of the aging experiment due to gas-phase photolysis of organic vapors under black UV lights. The SOA decrease is much more pronounced (~50%) during the experiment when particle-phase photolysis was added using the gas-phase rates. The corresponding loss rate due to the combined effect of gas- and particle-phase photolysis is 3.4×10^{-5} s^{-1}, which is within a factor of 2-3 of the values reported by Henry and Donahue (*2012*) and Wong et al. (*2014*).

These photolysis processes were parameterized in a global chemistry model, and the results suggest that condensed-phase photolytic reactions of organic aerosols could be an important loss process in the atmosphere, removing SOA from the troposphere on timescales of ~7 days which is comparable to those for wet deposition. In comparison, the gas-phase photolysis of semi-volatile organic compounds had a much smaller effect on SOA concentrations. We recognize that processes occurring inside the particle-phase (e.g oligomerization), which were not included in our study, can modify the chemical composition and properties of those chromophores, thus enhancing or reducing their ability to absorb radiation and undergo photolysis. These reactions

are still not well characterized (*Atkinson and Ziemann, 2012*) and are beyond the scope of this paper.

We note that the absorption by organic gases and/or particles is not expected to substantially affect the radiation field itself. Even in highly polluted conditions, aerosol optical depth (AOD) rarely exceeds 2, and only a fraction (1 minus the single scattering albedo (SSA)) is absorbed e.g. AOD=2 and SSA=0.9 gives an absorption optical depth of 0.2, corresponding to about 20% reduction in radiation. This is a significant but not overwhelming reduction, so that even under these highly polluted conditions the photochemistry is expected to proceed vigorously. Regional and global effects are expected to be smaller.

The implications of our results in terms of SOA modeling are twofold: (i) gas-phase photolysis of intermediate organic vapors which are currently ignored in most models, are likely to have a moderate impact on SOA yields over typical aerosol lifetimes in the atmosphere; (ii) in-particle photolysis could be a major sink for SOA if the quantum yields are substantial, and these need to be better constrained from measurements and included in 3D models. It is also worth noting that a substantial sink due to in-particle photolysis would imply that our current estimates of SOA formation rates would have to be revised upwards to be consistent with observed atmospheric SOA burdens. Finally, we note that a fuller understanding of ambient SOA formation rates will require a better understanding of SOA formation from other condensed-phase processes such as oligomerization and aqueous-phase chemistry.

Acknowledgements

We thank Dr. Andrew Conley (NCAR) for help with mathematical fitting, and Dr. Albert Presto (CMU) for providing the UV lamp spectrum. This research was supported by the National Center for Atmospheric Research, which is operated by the University Corporation for Atmospheric Research on behalf of the National Science Foundation, and by DOE (BER/ASR) grant DE-SC0006711. We would like to acknowledge high-performance computing support from

Yellowstone provided by NCAR's Computational and Information Systems Laboratory. Any opinions, findings and conclusions or recommendations expressed in the publication are those of the author(s) and do not necessarily reflect the views of the National Science Foundation. JLJ was partially supported by DOE (BER/ASR) DE-SC0011105.

532 **References**

533 Aumont, B., Valorso, R., Mouchel-Vallon, C., Camredon, M., Lee-Taylor, J., Madronich, S.
534 (2012), Modeling SOA formation from the oxidation of intermediate volatility n-alkanes, *Atmos.*
535 *Chem. Phys.*, 12, 7577-7589, 2012

536 Aumont, B., S. Szopa, and S. Madronich (2005), Modeling the evolution of organic carbon
537 during its gas-phase tropospheric oxidation: development of an explicit model based on a self
538 generating approach, *Atmos. Chem. Phys., 5,* 2497-2517.

539 Barnard, J. C., Volkamer, R., and Kassianov, E. I. (2008), Estimation of the mass absorption
540 cross section of the organic carbon component of aerosols in the Mexico City Metropolitan Area,
541 *Atmos. Chem. Phys., 8*, 6665–6679, http://www.atmos-chem-phys.net/8/6665/2008/.

542 Bey, I., Jacob, D.J., Yantosca, R.M., Logan, J.A., Field, B., Fiore, A.M., Li, Q., Liu, H., Mickley,
543 L.J. and Schultz, M. (2001), Global modeling of tropospheric chemistry with assimilated
544 meteorology: Model description and evaluation, *J. Geophys. Res.,* 106, 23,073-23,096.

545 Bones, D. L., Henricksen, D. K., Mang, S. A., Gonsior, M., Bateman, A. P., Nguyen, T. B.,
546 Cooper, W. J., and Nizkorodov, S. A. (2010). Appearance of strong absorbers and fluorophores in
547 limonene-O3 secondary organic aerosol due to NH+4 -mediated chemical aging over long time
548 scales, J. Geophys. Res.-Atmos., 115, D05203, doi:10.1029/2009JD012864.

549 Boucher, O., D. Randall, P. Artaxo, C. Bretherton, G. Feingold, P. Forster, V.-M. Kerminen, Y.
550 Kondo, H. Liao, U. Lohmann, P. Rasch, S.K. Satheesh, S. Sherwood, B. Stevens and X.Y. Zhang,
551 2013: Clouds and Aerosols. In: Climate Change 2013: The Physical Science Basis. Contribution
552 of Working Group I to the Fifth Assessment Report of the Intergovernmental Panel on Climate
553 Change [Stocker, T.F., D. Qin, G.-K. Plattner, M. Tignor, S.K. Allen, J. Boschung, A. Nauels, Y.
554 Xia, V. Bex and P.M. Midgley (eds.)]. Cambridge University Press, Cambridge, United Kingdom
555 and New York, NY, USA.

556 Denjean, C., Formenti, P., Picquet-Varrault, B., Camredon, M., Pangui, E., Zapf, P., et al. (2014).
557 Aging of secondary organic aerosol generated from the ozonolysis of α-pinene: effects of ozone,
558 light and temperature. *Atmos. Chem. Phys. Discuss.,* 14, 22437-22475.

559 Donahue NM, Henry KM, Mentel TF, Kiendler-Scharr A, Spindler C, Bohn B, Brauers T, Dorn
560 HP, Fuchs H, Tillmann R, Wahner A, Saathoff H, Naumann KH, Möhler O, Leisner T, Müller L,
561 Reinnig MC, Hoffmann T, Salo K, Hallquist M, Frosch M, Bilde M, Tritscher T, Barmet P,

562 Praplan AP, DeCarlo PF, Dommen J, Prévôt AS, Baltensperger U. (2012). Aging of biogenic
563 secondary organic aerosol via gas-phase OH radical reactions. *Proc. Natl. Acad. Sci. 21*,
564 109(34):13503-8. doi: 10.1073/pnas.1115186109.

565 Epstein, S.A., Blair, S.L., and Nizkorodov, S.A., (2014): Direct Photolysis of α-Pinene
566 Ozonolysis Secondary Organic Aerosol: Effect on Particle Mass and Peroxide Content, *Environ.*
567 *Sci. Technol.,* Article ASAP, DOI: 10.1021/es502350u.

568 Fann, N., Lamson, A.D., Anenberg, S.C., et al. (2012): Estimating the national public health
569 burden associated with exposure to ambient $PM_{2.5}$ and ozone, *Risk Anal* 32, 81–95.

570 Finlayson-Pitts, B. J.; Pitts, J. N. (2000), Chemistry of the upper and lower atmosphere: theory,
571 experiments, and applications; *Academic Press: San Diego*.

572 Graber, E. R. and Rudich, Y. (2006), Atmospheric HULIS: How humic-like are they? A
573 comprehensive and critical review, *Atmos. Chem. Phys.,* 6, 729-753, doi:10.5194/acp-6-729-
574 2006.

575 Henry, K.M. and Donahue, N.M. (2012): Photochemical Aging of α-Pinene Secondary Organic
576 Aerosol: Effects of OH Radical Sources and Photolysis, *J. Phys. Chem. A* 116 (24), 5932–5940.

577 Hodzic, A., Aumont, B., Knote, C., Lee-Taylor, J., Madronich, S., and Tyndall, G. (2014):
578 Volatility dependence of Henry's law constants of condensable organics: Application to estimate
579 depositional loss of secondary organic aerosols. *Geophysical Research Letters,* 41, doi:
580 10.1002/2014GL060649.

581 Jenkin, M.E., Saunders, S.M., Wagner, V., Pilling M.J. (2003): Protocol for the development of
582 the Master Chemical Mechanism, MCM v3 (Part B): tropospheric degradation of aromatic
583 volatile organic compounds, *Atmos. Chem. Phys.,* 3, 181-193.

584 Jo, D.S., Park, R.J., Kim, M.J., Spracklen, D.V. (2013): Effects of chemical aging on global
585 secondary organic aerosol using the volatility basis set approach, *Atmos. Environ., 81*, 230-244.

586 Knote, C., Hodzic, A., and Jimenez, J. L. (2015): The effect of dry and wet deposition of
587 condensable vapors on secondary organic aerosols concentrations over the continental US, *Atmos.*
588 *Chem. Phys.,* 15, 1-18, doi:10.5194/acp-15-1-2015.

589 Kwok, E.S.C., and R., Atkinson (1995): Estimation of hydroxyl radical reaction rate constants for
590 gas-phase organic compounds using a structure-reactivity relationship: an update, *Atmos.*
591 *Environ.,* 29,1685-1695.

592 Lambe, E. T., Cappa, C. D., Massoli, P., Onasch, T. B., Forestieri, S. D., Martin, A. T.,
593 Cummings, M. J., Croasdale, D. R., Brune, W. H., Worsnop, D. R., and Davidovits, P.:
594 Relationship between oxidation level and optical properties of secondary organic aerosol,
595 *Environ. Sci. Technol.,* 47, 6349–6357, 2013.

596 Lignell, H., Epstein, S.A., Marvin, M.r., Shemesh, D., Gerber, B., Nizkorodov, S. (2013):
597 Experimental and theoretical study of aqueous cis-pinonic acid photolysis. *J. Phys. Chem. A,* 117,
598 12930-12945.

599 Madronich, S. (1993), The atmosphere and UV-B radiation at ground level. *Environmental UV*
600 *Photobiology, Plenum Press,* 1–39.

601 Nannoolal, Y., Rarey, J., and Ramjugernath, D. (2008): Estimation of pure component properties:
602 Part 3. Estimation of the vapor pressure of non-electrolyte organic compounds via group
603 contributions and group interactions, *Fluid Phase Equilibria*, 269(1-2), 117-133, 2008.

604 Presto, A. A., Huff Hartz, K. E., Donahue, N. M. (2005): Secondary Organic Aerosol Production
605 from Terpene Ozonolysis 1. Effect of UV Radiation. *Environ. Sci. Technol.,* 39 (18), 7036−7045.

606 Salo K, et al. (2011). Volatility of secondary organic aerosol during OH radical induced ageing.
607 *Atmos Chem Phys,* 11, 11055–11067.

608 Schilling-Fahnestock, K. A., Yee, L. D., Loza, C. L., Coggon, M. M., Schwantes, R., Zhang, X.,
609 Dalleska, N. F., and Seinfeld, J. H.: Secondary Organic Aerosol Composition from C12 Alkanes,
610 *J. Phys. Chem. A*, doi:10.1021/jp501779w, 2014.

611 Shapiro, E. L., Szprengiel, J., Sareen, N., Jen, C. N., Giordano, M. R., and McNeill, V. F. (2009).
612 Light-absorbing secondary organic material formed by glyoxal in aqueous aerosol mimics,
613 Atmos. Chem. Phys., 9, 2289–2300, http://www.atmos-chem-phys.net/9/2289/2009/.

614 Spracklen, D.V., Jimenez, J.L., Carslaw, K.S., Worsnop, D.R., Evans, M.J., Mann, G.W., Zhang,
615 Q., Canagaratna, M.R., Allan, J., Coe, H., McFiggans, G., Rap, A. and Forster, P. (2011). Aerosol

mass spectrometer constraint on the global secondary organic aerosol budget. *Atmos. Chem. Phys. 11,* 12109–12136.

Tritscher T, et al. (2011). Volatility and hygroscopicity of aging secondary organic aerosol in a smog chamber. *Atmos. Chem. Phys.,* 11, 11477–11496.

Updyke, K. M., Nguyen, T. B., and Nizkorodov, S. A. (2012). Formation of brown carbon via reactions of ammonia with secondary organic aerosols from biogenic and anthropogenic precursors, Atmos. Environ., 63, 22–31.

Wong, J.P.S, Zhou, S., and Abbatt, P.D. (2014). Changes in Secondary Organic Aerosol Composition and Mass due to Photolysis: Relative Humidity Dependence. *J. Phys. Chem.* A, Article ASAP, DOI: 10.1021/jp506898c.

Zhang, J., Hartz, K. E. H., Pandis, S. N., and Dohanue, N. M.: Secondary organic aerosol formation from limonene ozonolysis: Homogeneous and heterogeneous influences as a function of NOx*, J. Phys. Chem., A*, 110, 11053-11063, 2006.

Zhong, M. and Jang, M.: Dynamic light absorption of biomass-burning organic carbon photochemically aged under natural sunlight (2014). Atmos. Chem. Phys., 14, 1517-1525, doi:10.5194/acp-14-1517-2014.

Ziemann, P. J. and Atkinson, R. 2012. Kinetics, Products, and Mechanism of Secondary Organic Aerosol Formation. *Chem. Soc. Rev.,* 41: 6582–6605.

Yee, L. D., Craven, J. S., Loza, C. L., Schilling, K. A., Ng, N. L., Canagaratna, M. R., Ziemann, P. J., Flagan, R. C., and Seinfeld, J. H. (2012): Secondary organic aerosol formation from low-NOx photooxidation of dodecane: Evolution of multigeneration gas-phase chemistry and aerosol composition, J. Phys. Chem. A, 116, 6211–6230, doi:10.1021/jp211531h.

Figures:

675 **Tables**

676 Table 1: Photolysis rate coefficients and photolytic lifetimes for typical atmospheric conditions
677 and for our simulations. Typical ozone overhead values are used at different locations based on
678 the Total Ozone Mapping Spectrometer data (http://disc.sci.gsfc.nasa.gov/acdisc/TOMS).

Typical Conditions		**Average J_{NO2} (s^{-1})**	**Average J_{O1D}(s^{-1})**	**Average $J_{NO3->NO2+O}$ (s^{-1})**
Boulder CO, summer solstice	40°N, sea level, June 21, $O_{3col.}$=310DU, 10% ground albedo, no aerosols, no clouds	4.1×10^{-3}	1.0×10^{-5}	9.1×10^{-2}
Boulder CO, winter solstice	40°N, sea level, Dec 21, $O_{3col.}$=330DU, 10% ground albedo, no aerosols, no clouds	1.5×10^{-3}	1.2×10^{-6}	4.6×10^{-2}
Equator June 21	Sea level, $O_{3col.}$=260DU, 5% ground albedo, no aerosols, no clouds	3.3×10^{-3}	1.0×10^{-5}	7.3×10^{-2}
Equator March 21	Sea level, $O_{3col.}$=258DU, 5% ground albedo, no aerosols, no clouds	3.6×10^{-3}	1.3×10^{-5}	7.8×10^{-2}
Hyytiala, summer solstice	61°N, June 21, $O_{3col.}$=355DU, 5% ground albedo, no aerosols, no clouds	4.3×10^{-3}	6.2×10^{-6}	1.0×10^{-1}
Hyytiala, winter solstice	61°N, Dec. 21, $O_{3col.}$=355DU, 90% ground albedo, no aerosols, no clouds	2.6×10^{-4}	5.8×10^{-8}	1.0×10^{-2}

Model Simulation		**Average J_{NO2} (s^{-1})**	**Average J_{O1D}(s^{-1})**	**Average $J_{NO3->NO2+O}$ (s^{-1})**	**Photolysis Age in J_{NO2} equivalent days**	
					Boulder, CO summer solstice	**Boulder, CO winter solstice**
GECKO-A 1 week simulations (Table 2)	40°N, 45° solar zenith angle, 7 days	8.1×10^{-3}	2.1×10^{-5}	1.8×10^{-1}	14 eq. days	38 eq. days
GECKO-A α-pinene ozonolysis SOA (Figure 6)	Black lights, 5 hours	3.0×10^{-3}	1.2×10^{-5}	2.1×10^{-3}	0.15 eq. days (3.7 eq. hours)	0.42 eq. days (10 eq. hours)
Henry and Donahue (*2012*)	Black lights, 5 hours	3.0×10^{-3}	-	-	0.15 eq. days (3.7 eq. hours)	0.42 eq. days (10 eq. hours)

679

680 Table 2: Description of GECKO-A simulations.

681

Experiments for SOA formed from α-pinene, toluene, C_{12},C_{16} n-alkane				
	Gas-phase photolysis of organics	Particle-phase photolysis	OH (molecules cm^{-3})	OA background ($\mu g\ m^{-3}$)
BASE	ON/OFF	OFF	$2x10^6$	10
SENS_OA	ON/OFF	OFF	$2x10^6$	1
SENS_OH	ON/OFF	OFF	$8x10^6$	1
$\boldsymbol{J_{molecmax(*)}}$	ON	ON as gas-phase J	$2x10^6$	10
$\boldsymbol{J_{mac}}$	ON	ON as 0.04% J_{NO2}	$2x10^6$	10

682 **(*)** Radical species that are produced by photolysis inside the particle are assumed to be
683 permanently lost to the gas-phase.

684

685

686 Table 3: Predicted reduction in SOA yields due to gas-phase photolysis, and corresponding first
687 order loss rates and lifetimes. The results are from the GECKO-A BASE case simulation, and
688 yields values are taken at the maximum of the SOA formation from each precursor. The loss rate
689 coefficients were estimated by numerically fitting the first order decay of SOA due to photolysis
690 occurring over one week of processing at constant light (J_{NO2}=$8.1x10^{-3}$ s^{-1}). Low (0.01 ppb) and
691 high (10 ppb) NOx simulations are shown.

Considered System	Reduction in SOA yields by gas-phase photolysis		Estimated loss rate (s^{-1})		Estimated lifetime (days, under simulation conditions*)	
	Low NOx	High NOx	Low NOx	High NOx	Low NOx	High NOx
α-pinene + OH	-16%	-47%	4.6×10^{-7}	2.1×10^{-6}	25.0	5.4
Toluene + OH	-11%	-13%	5.6×10^{-7}	4.3×10^{-7}	20.8	27.0
$C_{12}H_{26}$ + OH	-30%	-28%	1.2×10^{-6}	1.1×10^{-6}	9.3	10.4
$C_{16}H_{34}$ + OH	-10%	-13%	3.6×10^{-7}	3.7×10^{-7}	30.0	31.0

692 (*) To derive equivalent atmospheric loss rates (lifetimes) at mid-latitudes values should be
693 divided (multiplied) by a factor of 2 in summer and 5.4 in winter which is the ratio between J_{NO2}
694 used in our experiment and the typical atmospheric values.

695 Table 4: Estimated loss rates and lifetimes due to gas-phase and in-particle phase photolysis as
696 predicted by GECKO-A for the *Jmac* simulation over one week of aging at constant light
697 (J_{NO2}=8.1x10^{-3} s^{-1}).

Considered System	Estimated loss rate (s^{-1})		Estimated lifetime (days, under simulation conditions*)	
	Low NOx	High NOx	Low NOx	High NOx
α-pinene + OH	3.7×10^{-6}	5.6×10^{-6}	3.1	2.1
Toluene + OH	3.1×10^{-6}	1.1×10^{-6}	3.7	10.5
$C_{12}H_{26}$ + OH	4.7×10^{-6}	4.4×10^{-6}	2.5	2.6
$C_{16}H_{34}$ + OH	3.7×10^{-6}	3.5×10^{-6}	3.1	3.3

698 (*) To derive equivalent atmospheric loss rates (lifetimes) at mid-latitudes values should be
699 divided (multiplied) by a factor of 2 in summer and 5.4 in winter which is the ratio between J_{NO2}
700 used in our experiment and the typical atmospheric values.

Figures

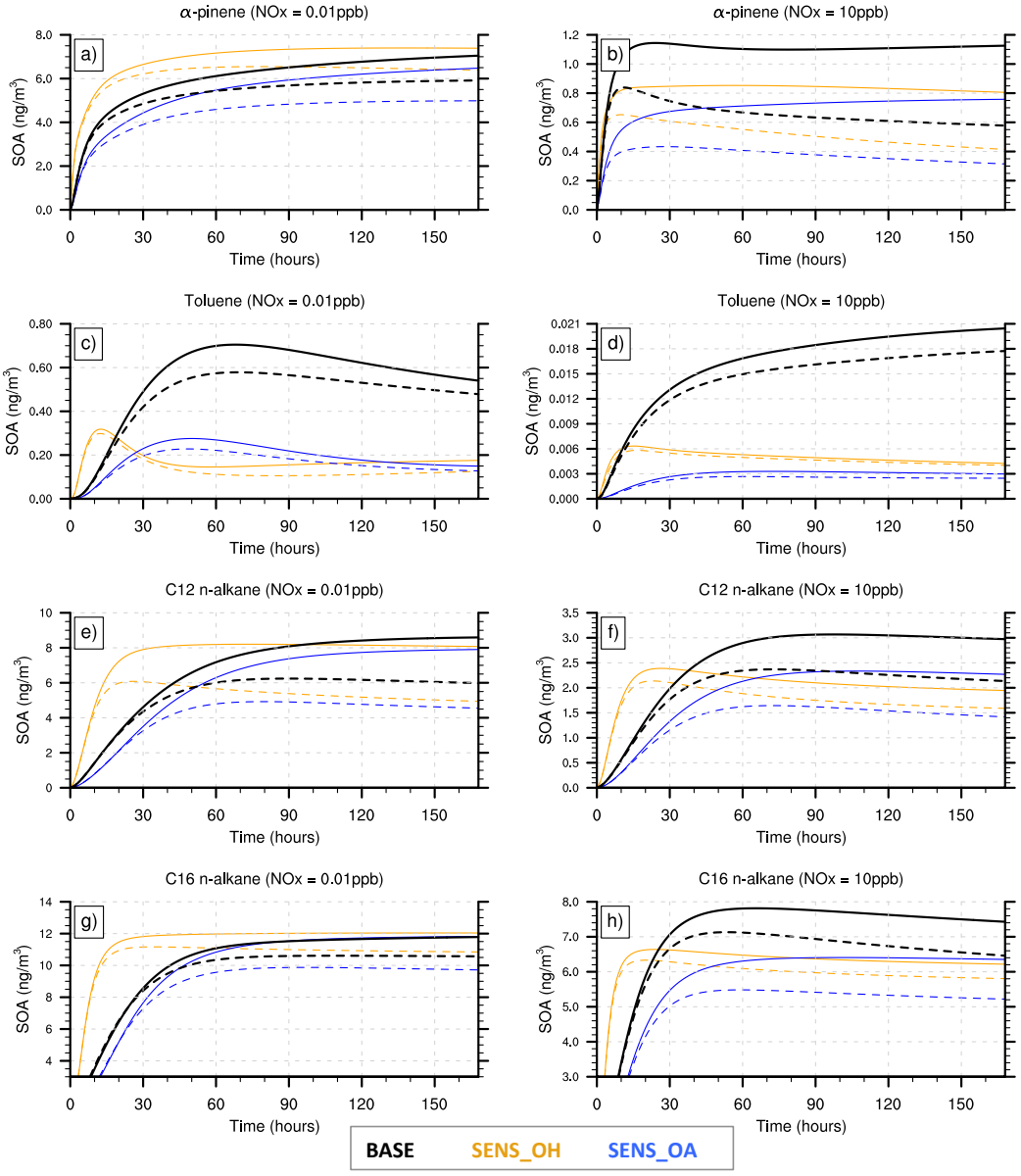

Figure 1: SOA formation from the oxidation by OH of 1 ppt of α-pinene, toluene, C_{12} and C_{16} n-alkanes at low (0.01 ppb) and high (10 ppb) NOx levels. Plots compare GECKO-A simulations with (dashed lines) and without (full lines) gas-phase photolysis of organics at the solar zenith angle of 45° (mid-latitudes) at constant daylight. To derive equivalent atmospheric summertime exposure of our experiment, the time axes should be multiplied by a factor of 2 (see Table 1). Reference simulation (BASE) is shown in black, and is compared to two sensitivity simulations testing for higher OH levels (SENS_OH in orange) and lower absorbing organic aerosol mass (SENS_OA in blue). See Table 2 for the description of various runs.

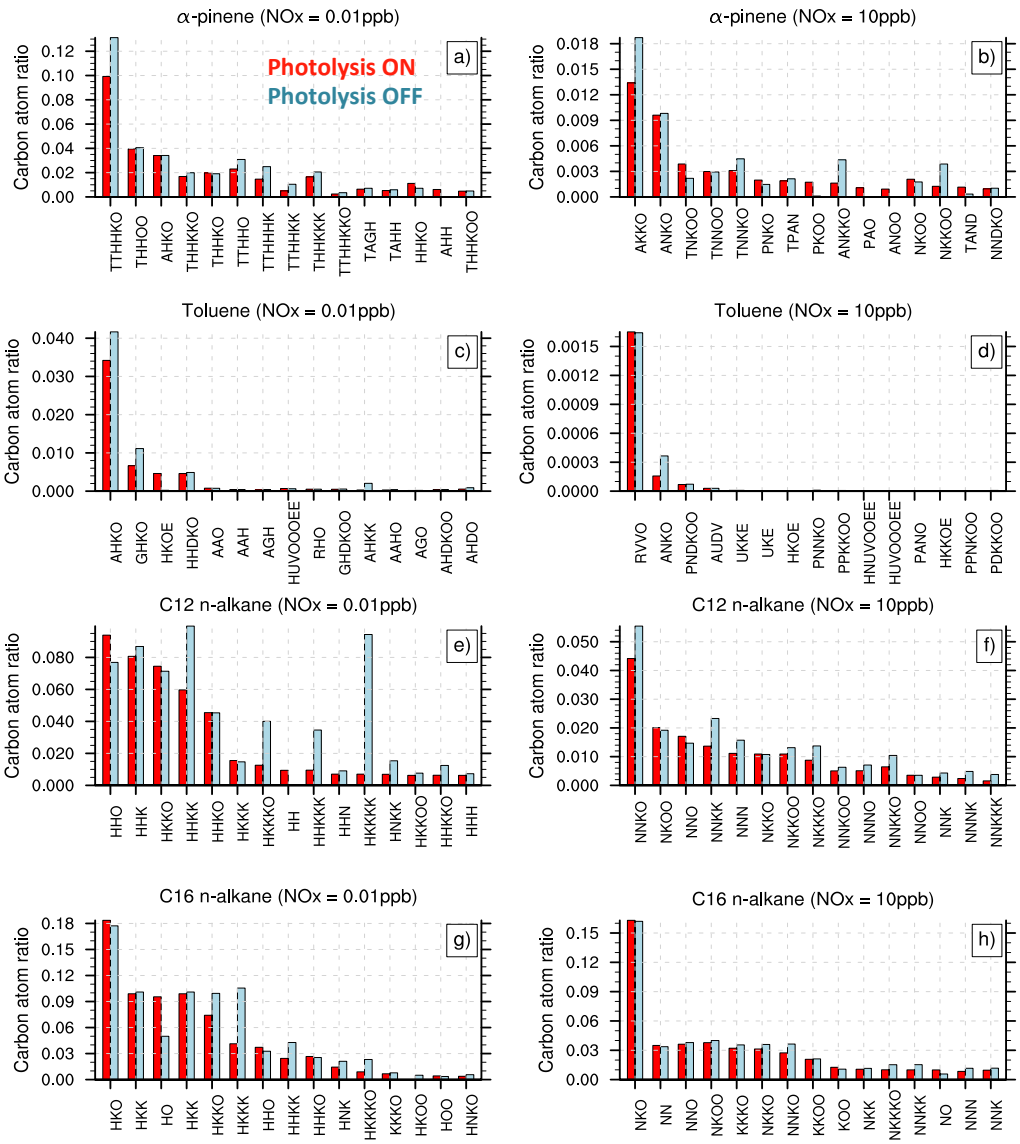

(A) Acid; (D) aldehyde; (H) hydroperoxide; (G) peracid; (K) ketone; (N) nitrate; (O) hydroxy; (P) PAN; (R) aromatic ring; (T) non-aromatic ring; (U) unsaturated; (V) = nitro

711

712 Figure 2: Particle-phase dominant functional groups in the top fifteen SOA constituents shown at
713 the maximum of the SOA yield. The BASE case simulations with (red bars) and without (blue
714 bars) photolysis of organic compounds are compared. The carbon atom ratio indicates the ratio of
715 the carbon atoms in the condensed phase to the initial carbon load included in the parent
716 backbone. The sum of the shown particle-phase constituents is lower than one as the rest of the
717 carbon mass is in the gas-phase.

718

719

720

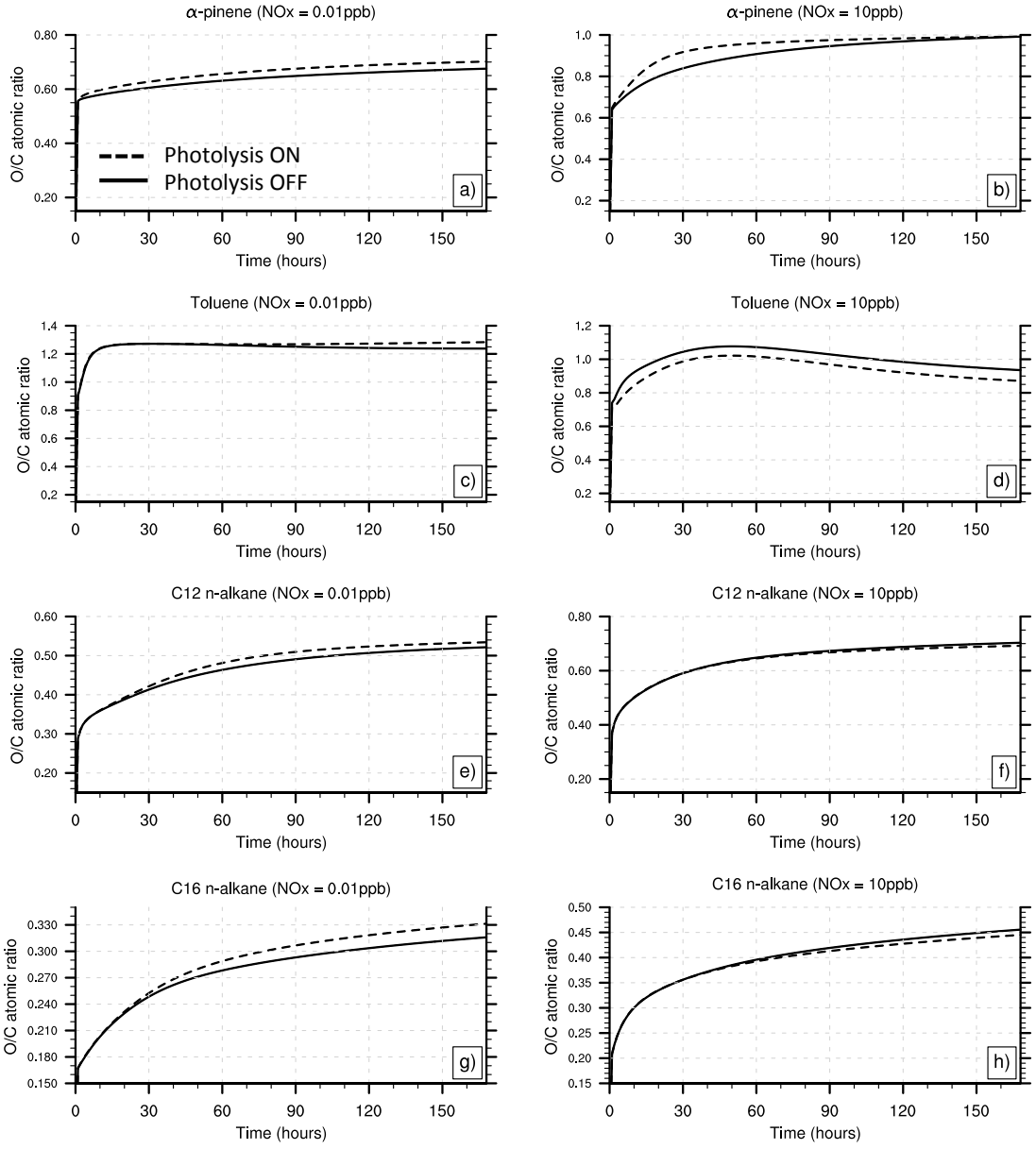

721

722 Figure 3: Oxygen to carbon (O/C) ratios as predicted by the BASE case simulation with (dashed
723 lines) and without (full lines) gas-phase photolysis of organics.

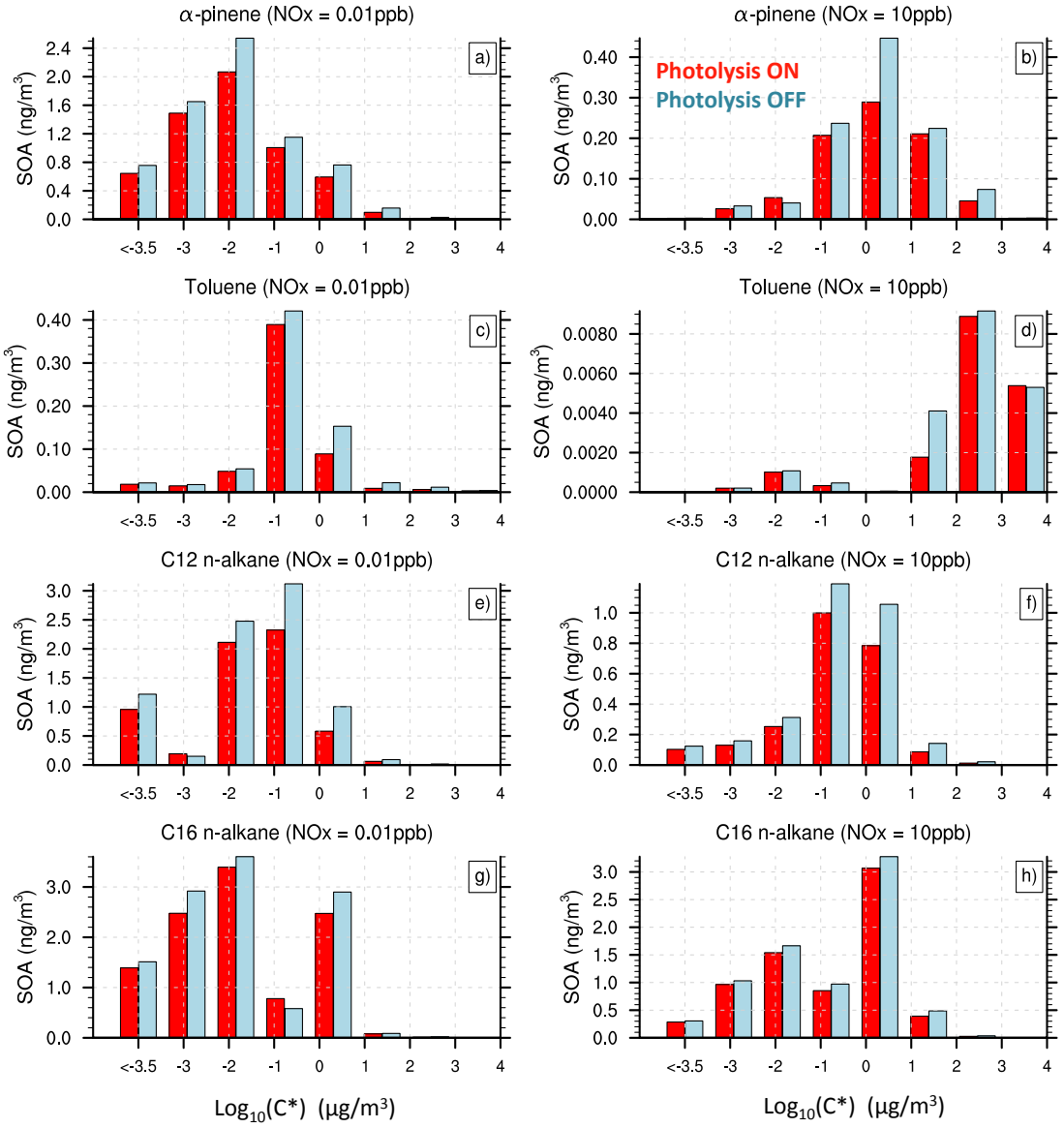

724

725 Figure 4: Distribution of products of OH oxidation of 1 ppt of α-pinene, toluene, C_{12} and C_{16} n-
726 alkanes at low (0.01 ppb) and high (10 ppb) NOx levels according to their volatility. The
727 volatility is expressed in terms of the effective saturation concentration (C*). Predictions
728 represent values at the maximum SOA yield based on the BASE case simulation with (red) and
729 without (blue) gas-phase photolysis of organics.

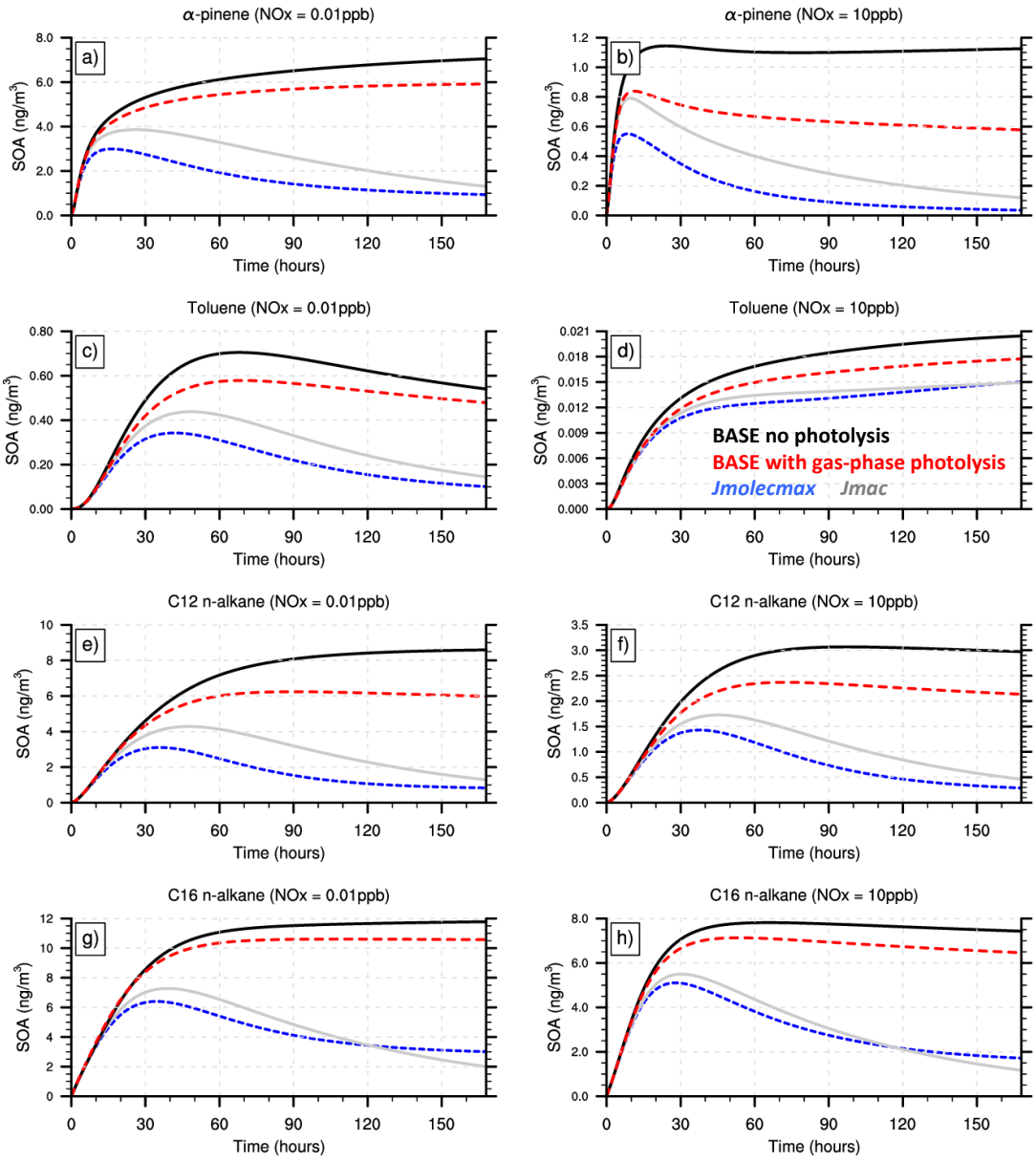

730

731 Figure 5: Predicted effect of photolysis on SOA concentrations from the oxidation of 1 ppt of α-
732 pinene, toluene, C_{12} and C_{16} n-alkanes at low (0.01 ppb) and high (10 ppb) NO_X levels. Plots
733 compare GECKO-A simulations for the BASE no photolysis run (black), BASE run with gas-
734 phase photolysis (red), $J_{molecmax}$ (blue) and J_{mac} (gray). To derive equivalent atmospheric
735 summertime exposure of our experiments, times should be multiplied by a factor of 2 (Table 1).
736 See Table 2 for the description of various runs.

737

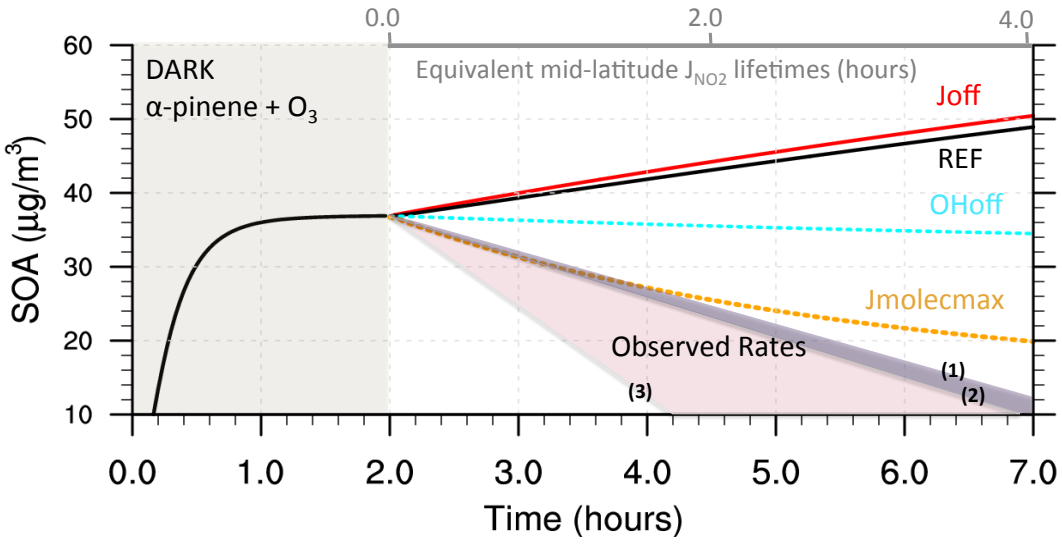

738

739 Figure 6: GECKO-A simulation of a typical SOA aging experiment. SOA is first made in the
740 dark in 2h from α-pinene ozonolysis in the conditions where the formation of hydroperoxides
741 dominates (through RO_2+HO_2 reactions). After the 2nd hour the initial precursor has been
742 consumed, and the SOA mixture is exposed to various conditions: (REF, black) UV black lights
743 and OH of 10^6 molecules cm^{-3}; (J_{off}, red) only OH oxidation with OH=10^6 molecules cm^{-3} and
744 photolysis are turned off for organic compounds; (OH_{off}, cyan blue) only UV black lights;
745 ($J_{molecmax}$, orange) similar to the REF case, but the photolysis of organic molecules is performed
746 also in the condensed phase. The UV lamp is that of Presto et al. (2005), with J_{NO2}=3x10^{-3} s^{-1},
747 NOx levels are kept at 0.01 ppb, and ozone levels are set at 50ppb during the aging simulations.
748 SOA loss rates reported in the experiments are also shown in shaded purple areas with slopes
749 corresponding to (1) Henry and Donahue (*2012*) (6×10^{-5} s^{-1}), (2) Wong et al. (*2014*) for dry
750 conditions (7.9×10^{-5} s^{-1}) and (3) Wong et al. (*2014*) for humid conditions (1.6×10^{-4} s^{-1}).

751

752

753

754

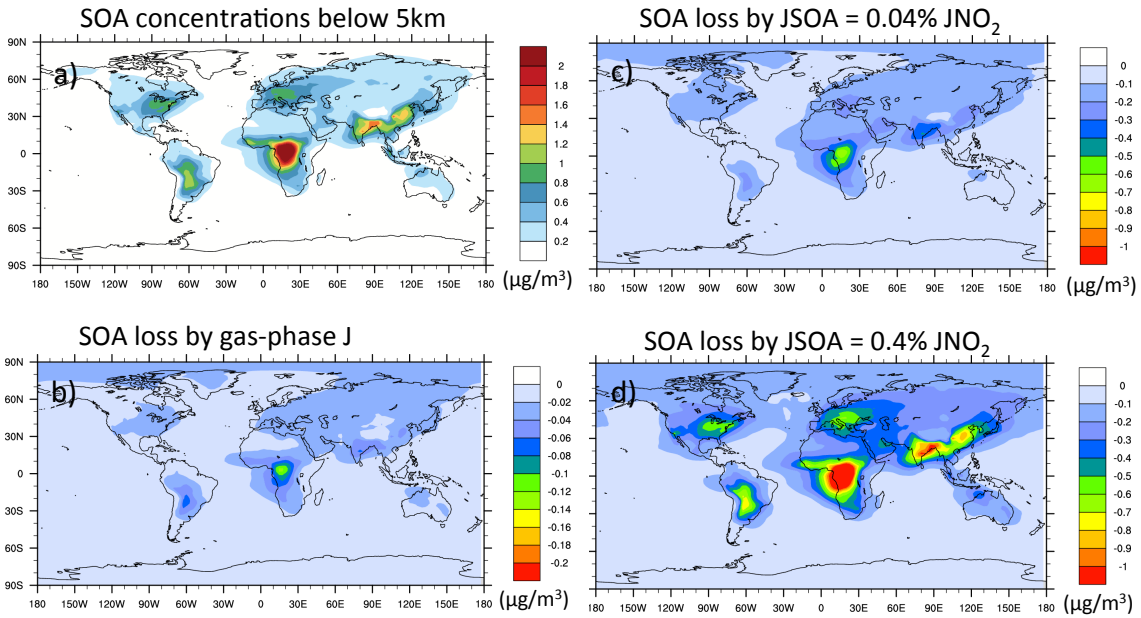

Figure 7: GEOS-Chem simulation for 2009 showing (a) the SOA concentrations within the lower troposphere (below 5km), and the absolute (µg m^{-3}) reductions in SOA concentrations due to gas-phase (b) and particle-phase (c, d) photolysis. Gas-phase photolysis is applied to semi-volatile organic compounds using the e-folding J lifetime of 20 days as estimated in Table 3. Two in-particle photolysis rates are considered i.e. J_{SOA} of 0.04% J_{NO2} (c), and J_{SOA} of 0.4% J_{NO2} (d).

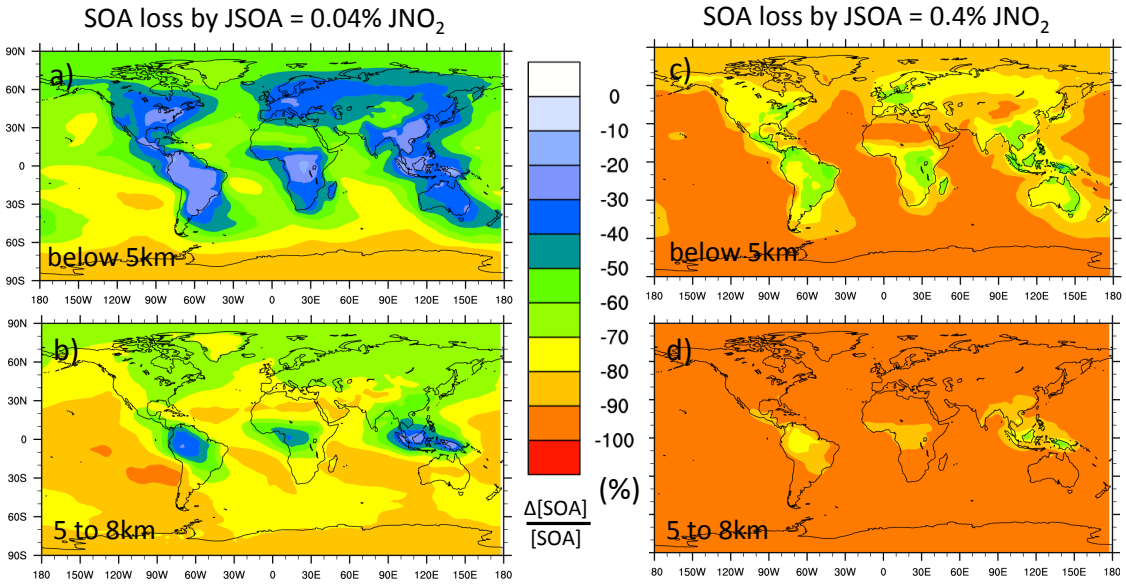

Figure 8: Relative reductions (%) in SOA concentrations due to particle-phase photolysis in the lower (a, c) and upper (b, d) troposphere. Two in-particle photolysis rates are considered i.e. J_{SOA} of 0.04% J_{NO2} (left side), and J_{SOA} of 0.4% J_{NO2} (right side).